Fuel 263 (2020) 116743

Contents lists available at ScienceDirect

Fuel

journal homepage: www.elsevier.com/locate/fuel

Full Length Article

Effects of molar expansion ratio of fuels on engine efficiency

Duc-Khanh Nguyen[a,*], James Szybist[b], Louis Sileghem[a], Sebastian Verhelst[a,c,*]

[a] Department of Electrical Energy, Metals, Mechanical Constructions and Systems, Ghent University, Belgium
[b] Fuels, Engines, and Emissions Research Center, Oak Ridge National Laboratory, TN, United States
[c] Department of Energy Sciences, Lund University, Sweden

ARTICLE INFO

Keywords:
Molar expansion ratio
Fuel properties
Spark-ignition engines
Energy losses
Engine efficiency

ABSTRACT

Fuel properties have a strong impact on the efficiency of internal combustion engines. Contrary to other physical and thermochemical fuel properties, the molar expansion ratio is normally ignored. Molar expansion ratio is the ratio of number of moles of the products to the reactants. In this work, the impact of the fuel's molar expansion ratio on engine efficiency is investigated. Findings are based on simulations of a spark ignition engine using different fuels (standard fuels and user-defined fuels) and different dilution ratios. Simulations without heat transfer and friction were performed first. The combustion then takes place at top dead center with a very short combustion duration to approach the ideal Otto cycle. The heat transfer and friction were then added step by step. From this analysis, it could be concluded that the heat loss and friction work decrease as molar expansion ratio increases. The gross indicated and brake thermal efficiencies thus increase. User-defined fuels with different molar expansion ratio, but the same physical and thermochemical properties were then employed. The simulated results showed that the brake thermal efficiency increases by around 1.15% with an increase in molar expansion ratio of 0.02 compared to a fuel with a molar expansion ratio of unity. The simulation was also done with air and exhaust gas recirculation dilution.

1. Introduction

Improving the thermal efficiency of spark-ignition (SI) engines is important to meet the future CO_2 emissions legislation. Besides the use of advanced engine technologies such as variable valve timing, cylinder deactivation, Miller/Atkinson cycle, water injection, etc. [1], fuel properties play an important role in engine efficiency. The three key properties which have the strongest impact on SI engine efficiency include anti-knock quality, the heat of vaporization (HoV), and laminar burning velocity (LBV) [2]. Practically, other fuel's properties are important such as energy density, ease of storage and distribution, material compatibility, or non-conventional emissions, etc. However, engine efficiency is one of the most important focus areas currently.

The compression ratio (CR) in SI engines is limited by knock. Knock is the auto-ignition of the end gas at high pressure and temperature, before it can be consumed by the flame front. A fuel with high anti-knock quality enables to operate under higher CR, so engine efficiency increases. The knock resistance of a fuel normally is indicated by the Octane numbers [3], Research Octane number (RON) [4] and Motored Octane number (MON) [5]. If two fuels have the same RON, a lower MON fuel has a better performance on the mitigation of knock under boosted operating conditions and thus higher engine efficiency [6–10]. The auto-ignition strongly depends on the temperature of the end gas. Therefore, a fuel with high HoV has a better knock resistance. Furthermore, a reduction in unburned gas temperature due to fuel evaporation helps to reduce the combustion temperature, so heat loss decreases.

The heat loss also depends on the combustion duration and phasing. A shorter combustion duration might cause an increase in heat transfer due to higher maximum temperature and peak pressure. However, the effective expansion ratio and degree of constant volume combustion increase. Thus, engine efficiency normally increases with faster combustion. Cracknell et al. [11] concluded that faster burning fuels can lead to a more optimum combustion phasing, resulting in a more efficient engine. Other studies also confirmed that faster burning fuels can improve the dilution tolerance in SI engines, allowing engine efficiency increases through increased dilution [12–14]. Recently, Miles [2] has developed a merit function to calculate the relative efficiency benefit of a fuel compared to gasoline. A fuel (blend) with high RON, low MON, high HoV and high LBV results in an increase in the merit function score.

In that merit function, the molar expansion ratio (MER) is neglected. The MER is defined as the ratio of the number of moles of products to the reactants. For example, hydrogen has a MER less than unity, and

* Corresponding authors.
E-mail addresses: duckhanh.nguyen@ugent.be (D.-K. Nguyen), sebastian.verhelst@energy.lth.se (S. Verhelst).

https://doi.org/10.1016/j.fuel.2019.116743
Received 8 August 2019; Received in revised form 15 October 2019; Accepted 23 November 2019
Available online 06 December 2019

iso-octane has a MER greater than unity. Although this is a less explored fuel property, it is an important one. MER determines the extent of residual pressure available to do useful work. This is evident in the ASTM measurement of lower heating value (LHV) [15], which uses a constant volume chamber to burn the fuel in a pure oxygen environment, then cools the combustion products so that the initial and final temperatures are nearly identical. In this scenario, if the MER is unity, the final pressure is the same as the initial pressure and there is no remaining potential to perform work. However, where MER is greater than unity, the final pressure in the constant volume chamber is greater than the initial pressure, representing the potential to perform additional work. Conversely, where MER is less than unity, the final pressure is less than unity.

Previously, Szybist et al. [16] concluded that an engine is able to produce a higher output with a fuel that has a higher MER. Nguyen et al. [17] also confirmed the importance of MER on engine efficiency for the case of fuel reforming using waste exhaust heat. A low MER of the fuel reformates (H_2 and CO) was shown to cause a smaller improvement in the output than could be expected by the increase of lower heating value. However, both studies limited the analysis of MER's effect to the Otto cycle efficiency. The impact of MER on various energy losses has not been studied yet.

In this work, the impact of the MER on energy losses and engine efficiency will be analyzed. The engine cycle with and without energy losses was simulated using GT-Power [18]. Standard fuels, as well as user-defined fuels, were employed to evaluate the influence of the MER on engine efficiency, initially for a non-diluted condition. Air and exhaust gas recirculation (EGR) dilution then were investigated for the cases of hydrogen and iso-octane. Based on this research, a recommendation about future fuel designs will be made. It could also provide a better estimation of the tank-to-wheel efficiency for such new fuels.

2. Research methodology

In order to evaluate the influence of the MER, first the equation to calculate the MER for different fuels and different dilution ratios was written. The combustion reaction for a general fuel $C_xH_yO_z$ for equivalence ratio (ϕ) less than or equal to unity (stoichiometric and lean conditions) and different EGR ratio (Y_{egr}) is presented in reaction (R1).

$$C_xH_yO_z + \frac{d}{\phi}(O_2 + 3.76N_2) + Y_{egr}\left[aCO_2 + bH_2O + cN_2 + d\left(\frac{1}{\phi} - 1\right)O_2\right] \rightarrow aCO_2 + bH_2O + cN_2 + d\left(\frac{1}{\phi} - 1\right)O_2 \quad \text{(R1)}$$

Coefficients a, b, c, and d in reaction (R1) can be calculated as a function of x, y, z, ϕ, and Y_{egr}. Based on that, the MER can be expressed as in Eq. (1).

$$MER = \frac{4.76\left(x + \frac{y}{4} - \frac{z}{2}\right) + \left(\frac{y}{4} + \frac{z}{2}\right)[\phi + Y_{egr}(1 - \phi)]}{4.76\left(x + \frac{y}{4} - \frac{z}{2}\right) + \left[1 - Y_{egr}\left(1 - \frac{y}{4} - \frac{z}{2}\right)\right][\phi + Y_{egr}(1 - \phi)]} \quad (1)$$

As can be seen in Eq. (1), MER is influenced by the fuel's chemical formula (x, y and z) and the dilution ratio (Y_{egr} and ϕ). When diluted, MER approaches unity with an increase of dilution fraction (an increase of Y_{egr} and a decrease of ϕ). In order to see the impact of MER, simulations were performed for different fuels without dilution first, after which the impact of MER due to the increase of dilution fraction will be studied. First, the simulation approach will be explained.

2.1. Simulation approach

The study will begin with an ideal Otto cycle, for different fuels, without dilution. The Otto cycle efficiency is determined by dividing the Otto mean effective pressure (Otto MEP) by the fuel mean effective pressure (FuelMEP). FuelMEP is calculated as a ratio of fuel energy (or inlet energy), on the basis of the LHV, to the engine displacement volume [19]. Then, the energy losses such as due to combustion phasing, combustion duration, heat loss and friction loss are added. The simulation was performed on a single cylinder engine from −180 to +180 CAD aTDC (after top dead center), without gas exchange. Therefore, the impact of pumping mean effective pressure (PMEP) is not considered in this work. After taking the other losses into account, the "gross" brake mean effective pressure (BMEP) can be calculated. The gross BMEP is given by Eq. (2).

$$grossBMEP = BMEP - PMEP \quad (2)$$

Initial pressure and initial temperature (at −180 CAD aTDC) were set at 1 bar (as approximately the case for naturally aspirated SI engines at wide open throttle) and 40 °C, respectively. Due to a constant intake pressure, the fuel energy and engine load vary. With this high intake pressure, PMEP is very small. In this work, the pumping work is therefore neglected, thus gross BMEP equals BMEP. In practice, PMEP might increase with MER. Because of a higher combustion pressure, the cylinder pressure after the expansion and consequently exhaust pressure slightly increases.

The geometry of a Volvo T3 engine was used for this study [20]. It is a four cylinder SI engine with a swept volume of 1.6 liters, a compression ratio of 10:1, a bore of 79 mm and a stroke of 81.4 mm. In this work, only one cylinder was simulated. The recommended wall temperatures from GT-Power were employed for all simulations [18]. The engine speed was fixed at 1500 rpm.

An additional simulation with a higher compression ratio, 12:1, was performed to see the interaction between MER and compression ratio.

The cycle starts with an air-fuel mixture at the initial condition, 1 bar and 40 °C, from bottom dead center. Although the Volvo T3 is a direct-injection SI engine [20], the liquid fuel was assumed to be fully vaporized before compression. Therefore, the impact of the fuel's HoV is ignored. This effect will be discussed separately in future work.

Then, the mixture is compressed to a higher pressure before starting the combustion. Differences in specific heat ratio of the working fluid causes a difference in motored pressure and temperature. More complex fuels (higher MER fuels, see later) have a higher degree of freedom in terms of vibrational and rotational states (e.g. H_2 has only two rotational degrees of freedom, lower than more complex fuels), which causes an increase in specific heat and a decrease in specific heat ratio.

Fig. 1 shows the cylinder pressure-temperature trajectories for the stoichiometric mixture of four selected fuels (hydrogen, methane, propane, and iso-octane) during the compression stroke. At the beginning of the compression, all fuel-air mixtures have the same pressure and temperature. However, there is a difference in the cylinder pressure and especially the unburned gas temperature at the end of the compression. Lower MER fuels (lower heat capacity and higher specific heat ratio, see Section 3) have a higher unburned gas temperature [21]. As can clearly be seen, the difference in unburned gas temperature at the end of compression between hydrogen and iso-octane is obvious, around 100 K. The difference in cylinder pressure is around 3 bar.

Pressure (p) and unburned gas temperature (T) for the adiabatic compression process can be estimated as a function of initial pressure/temperature (p_0, T_0), compression ratio (CR) and specific heat ratio (γ), as in Eq. (3). As can be seen, the difference in γ between these fuels results in a difference in final pressure. The difference in temperature is caused by the difference in $(\gamma - 1)$ between the fuels. The relative difference in $(\gamma - 1)$ between the fuels is more obvious than the relative difference in γ. This explains for a bigger difference in temperature than in pressure between these fuels at the end of compression, as shown in

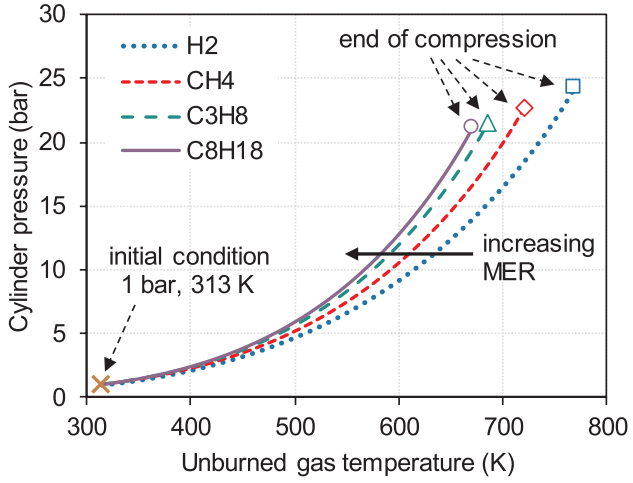

Fig. 1. In-cylinder pressure-temperature trajectories for four selected fuels during the compression.

Fig. 1.

$$p = p_0(CR)^{\gamma}$$
$$T = T_0(CR)^{(\gamma-1)} \quad (3)$$

At the end of the compression stroke, in order to simulate the combustion, the Wiebe function was employed to represent the heat release profile. The mass fraction burned is thus described by Eq. (4) [22]:

$$x_b = 1 - exp\left[-a\left(\frac{\theta - \theta_0}{\Delta\theta}\right)^{w+1}\right] \quad (4)$$

where $\Delta\theta$ and θ_0 are set by matching the desired combustion phasing CA50 (50% mass fraction burned) and combustion duration CA10-90 (10–90% burn duration). The efficiency factor a in Eq. (4) is fixed at 5 and the shape parameter w is calibrated to minimize the error in burning rate versus experiment. This just serves as a starting case. The measured burning rate in the selected engine was employed to calibrate the Wiebe model. Fig. 2 presents the comparison of mass fraction burned profiles from experiment and simulation (at two values of w) with the same CA50 and CA10-90 as an experiment [20]. A shape factor w of 2 is suggested by Heywood [22], which provides quite a good agreement. However, the burning rate from the simulation is better matched with the experiment with $w = 1.42$. Thus, that value is employed for all simulations. Combustion efficiency (chemical energy

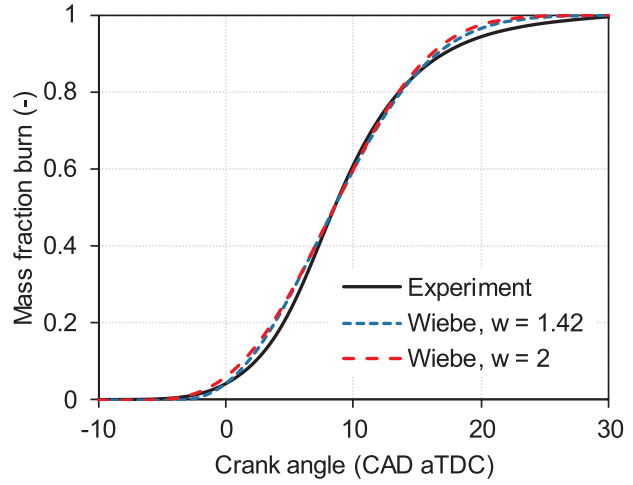

Fig. 2. Comparison of mass fraction burned from experiment [20] and Wiebe combustion model with $w = 1.42$ and $w = 2$.

conversion) is taken to be 100%. Effects of CO_2 and H_2O dissociation are not considered.

The purpose of using a simplified combustion model is to allow easy control of combustion duration and combustion phasing. The combustion phasing and combustion duration have a strong impact on heat transfer, friction, and consequently brake efficiency. Also, the laminar burning velocity and Lewis number are fuel dependent, so the difference in brake efficiency might be the result of a difference in combustion duration and combustion phasing if a more complex combustion model was employed. The effect of MER then becomes less dominant. The simplified combustion model was thus chosen in order to isolate the impact of MER on brake efficiency.

The heat loss Q can be estimated as in Eq. (5), where *htm* is the heat transfer multiplier, A is the heat transfer area, h is the heat transfer coefficient, T_{gas} is the in-cylinder gas temperature and T_{wall} is the wall temperature. The heat transfer coefficient from Morel & Keribar's model [23] was used because this model takes the impact of in-cylinder flow field into account. When simulating a cycle without heat loss, a *htm* of 0 was employed. For a *htm* of 1 (standard settings), the heat loss is 100% as determined using the model of Morel and Keribar. The heat transfer loss mean effective pressure (HTMEP) then can be easily calculated with heat loss Q and engine displacement volume [19].

$$Q = htm \times Ah(T_{gas} - T_{wall}) \quad (5)$$

The friction mean effective pressure (FMEP) is predicted following Chen & Flynn's expression, as in Eq. (6) [24]. FMEP (in bar) is thus predicted as a function of the friction multiplier *fm*, the mean piston speed U_p (in m/s) and the peak in-cylinder pressure P_{max} (in bar). For an *fm* of 0, the mechanical friction equals zero. If the friction is taken into account, *fm* equals 1.

$$FMEP = fm \times [0.4 + 0.005P_{max} + 0.09U_p + 0.0009U_p^2] \quad (6)$$

To simulate the Otto cycle, a very short combustion duration is used to represent constant volume combustion. A CA10-90 duration of 2 CAD [25] and a CA50 location at the top dead center [26] are employed. The *htm* and *fm* were set to 0 in this case. After the "Otto cycle calculations", the heat loss and friction loss were added for more realistic cycles, i.e. *htm* and *fm* equal 1. The constants used to determine heat and friction losses in Eqs. (5) and (6) were kept constant across all of the fuels investigated.

With a constant volume combustion in the Otto cycle, the peak pressure and maximum temperature are high, which results in increased HTMEP and FMEP when these effects are included, thus BMEP decreases. CA50 and CA10-90 were therefore varied in a matrix (with steps of 0.25 CAD) to find the optimum values leading to the maximum BMEP. With a finite combustion duration, the HTMEP and FMEP decrease, so the BMEP is higher compared to the BMEP with constant volume combustion.

There are some assumptions and several models were used. Employing other sub-models might cause different results. In this work, no pumping loss was assumed. In practice, MER might have a small impact on the pumping work. Thank to a higher maximum pressure with high MER fuel, the pressure at the end of expansion (or at exhaust valve opening) will be slightly higher. This might result in a higher pumping work. Furthermore, the wall temperature was fixed in this work. In fact, the combustion temperature is not the same for all fuels, so the wall temperature might have a bit difference.

In practice, the combustion phasing is easily controlled by changing the ignition timing to achieve the optimum CA50. Combustion duration, CA10-90, is dependent on many factors that are not associated with MER, such as laminar burning velocity, diffusivity, and turbulence. However, in order to isolate the effect of MER, the optimum CA10-90 was employed. The effects of the fuel's laminar burning velocity, diffusivity, and in-cylinder turbulence on combustion duration were not considered in this work. The simulation approach for non-

Table 1
Key properties of standard fuels and user-defined fuels.

Properties	Standard fuels							User-defined fuels	
								Option 1	Option 2
Formula	H_2	CH_4	C_2H_6	C_3H_8	C_4H_{10}	C_7H_{16}	C_8H_{18}	C_nH_{2n}	C_nH_{2n}
MER (–)	0.852	1	1.028	1.04	1.047	1.056	1.058	= f(n)	= f(n)
MW (g/mol.)	2	26	30	44	58	100	114	= f(n)	= f(n)
LHV (MJ/kg)	119.9	50	47.5	46.4	45.7	44.6	44.3	44.6	varies
A/F_{st} (kg/kg)	34.3	17.15	16.01	15.59	15.38	15.09	15.05	14.7	14.7
A/F_{st} (v/v)	2.38	9.52	16.66	23.8	30.94	52.36	59.5	= f(n)	= f(n)

diluted mixtures will be presented first, then the approach for diluted cases will be shown.

2.2. Non-diluted combustion

When simulating non-diluted operation, the working fluid consists of a stoichiometric mixture of fuel and air, without dilution (no excess air, residual, or external EGR). “Standard fuels” from the GT-Power fuel database were employed. Fuels with a chemical formula of C_nH_{2n+2}, with n varying from 0 to 8 (i.e., H_2 and C1-C8 alkanes), were employed. The reason why this fuel class was chosen is the huge variety in MER. Over this range, the MER increases from 0.852 (for hydrogen, $n = 0$) to 1.058 (for iso-octane, $n = 8$). Table 1 presents the key properties of these standard fuels. MER can be seen to increase for a more complex fuel.

This modeling investigation assumes that all of the fuels are pre-mixed in the gas phase. Due to a difference in the fuel’s molecular weight with varying n in its chemical formula, the density of the fuel and fuel-air mixture changes. Density (ρ) of an ideal gas can be calculated as in Eq. (7).

$$\rho = \frac{P.\ MW}{R.\ T} \tag{7}$$

where P is the pressure, MW is the molecular weight, R is the gas constant, and T is temperature.

The fuel’s density changes proportionally to a change of molecular weight. Thus, the fuel’s density increases as MW (and MER) increases. The volume fraction of fuel and air in the cylinder depends on the volume based A/F_{st}. A more complex fuel has a higher volumetric A/F_{st}, therefore the volume fraction of that fuel is smaller. If two fuels have the same density, the air-fuel mixture for the more complex one (higher MER) has a lower density due to the lower volume fraction of fuel in the mixture.

Fig. 3 shows the molecular weight and volume based A/F_{st} as a function of MER for the standard fuels. As can clearly be seen, the increase of MW (or density) is more obvious than the enhancement of the volume based A/F_{st} (for C_nH_{2n+2} class), so the density of the air-fuel mixture increases as MER increases. These fuels also have different lower heating value (LHV) and stoichiometric air-to-fuel ratio (A/F_{st}). User-defined fuels, therefore, were also employed to better isolate the impact of MER.

To define a new fuel in GT-Power, the *FluidGas* template was used. Several properties of gases and/or vapors such as the number of carbon/hydrogen/oxygen atom in each molecule, LHV, critical temperature/pressure, enthalpy coefficients, etc. can be defined by the users with this template. In this work, fuels with the same properties as n-heptane were defined (e.g. LHV, enthalpy coefficients, and so on). In order to have different MER, the number of carbon/hydrogen atoms per molecule was varied. The chemical formula of C_nH_{2n} (with n varying from 2 to 10) was chosen because of a nearly constant A/F_{st}, of about 14.7, so the impact of A/F_{st} can then also be ignored. MER increases from 1 (for C_2H_4) to 1.055 (for $C_{10}H_{20}$). Although these user-defined fuels have the chemical formula of alkenes, these fuels are not “actual” alkenes in terms of properties.

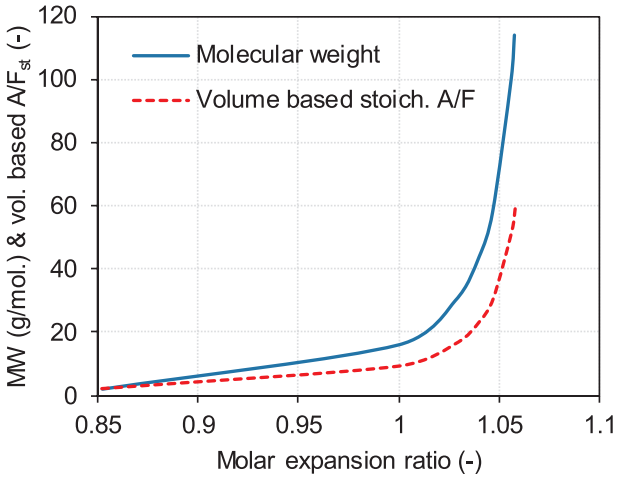

Fig. 3. Molecular weight and volume-based stoichiometric air-to-fuel ratio of standard fuels as a function of molar expansion ratio.

Because of the fact that the user-defined fuels have the same mass based A/F_{st}, this results in increased fuel mass for higher MER fuels due to the increase of the fuel’s density. Furthermore, the LHV is fixed, thus the inlet energy is not identical for all fuels. A second option for user-defined fuels, therefore, was considered: the LHV was varied from fuel to fuel, to maintain the inlet energy, which is represented in the second column for user-defined fuels in Table 1. A higher MER fuel then has a lower LHV. The LHV of the “reference fuel”, C_2H_4, was set at 44.6 MJ/kg, as n-heptane, similar to the first option.

In this work, all studied candidates (standard and user-defined fuels) are non-oxygenates, chosen for the big difference in MER and the fixed stoichiometric A/F ratio. Section 4.4 extends the discussion for the case of oxygenates.

2.3. Diluted combustion

In order to ascertain the effects of dilution, both lean and stoichiometric EGR dilution are explored for two fuels: hydrogen and iso-octane. These fuels were chosen because of the huge difference in MER between the two fuels: 0.852 for hydrogen and 1.058 for iso-octane. The purpose here is the comparison between air and EGR dilution for a specific fuel, thus no simulations with user-defined fuels were performed to explore this dilution effect. The working fluid is either diluted by air (lean combustion) or by the burned gases (or EGR). In order to compare two kinds of dilution, the fuel-to-charge equivalence ratio ϕ' was used, defined in Eq. (8) [27].

$$\phi' = \frac{F/(A+R)}{F/A_{st}} = \phi\left(\frac{1-Y_{egr}}{1+\phi Y_{egr}(F/A)_{st}}\right) \cong \phi(1-Y_{egr}) \tag{8}$$

According to Lavoie et al. [27,25], ϕ' is a measure of the specific

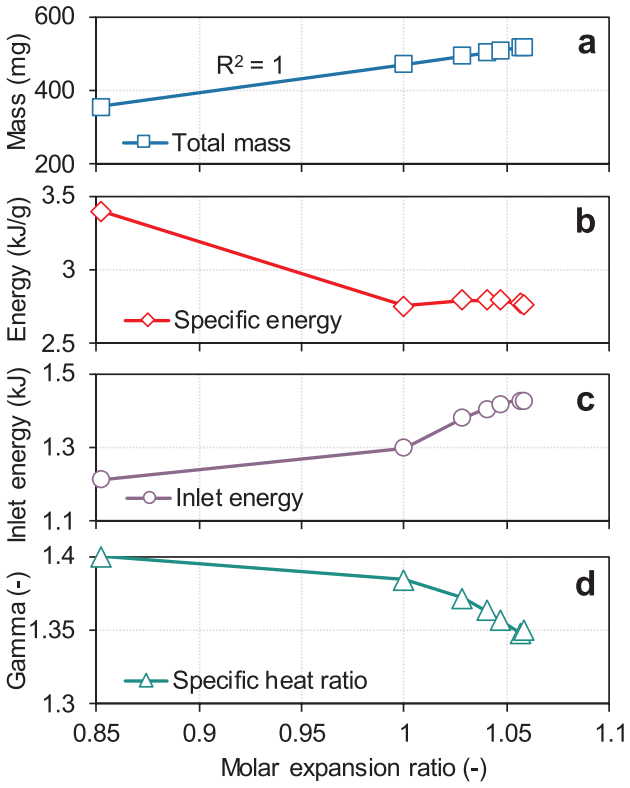

Fig. 4. Total reactant mass, specific reactant energy, inlet energy and specific heat ratio of standard fuel-air mixtures as a function of molar expansion ratio.

energy content of the charge. Three values of ϕ' were tested ($\phi' = 0.8, 0.6, 0.4$). The MER tends towards unity with increased dilution levels, or decreased ϕ'. As shown in Reaction R1, the EGR mixture was simplified as a mixture of completed combustion products such as CO_2, H_2O and N_2. In practice, NO in the exhaust gas can have a strong effect on the ignition delay. However, engine knock was not considered and the combustion event was defined by the Wiebe function, thus the ways in which NO could be important are neglected in this study.

3. Working fluid properties

In this section, properties of the working fluid or the reactant for both non-diluted and diluted cases will be discussed. Working fluid properties influence the compression process, combustion, heat transfer, and friction. Thus, an understanding of these properties is needed to explain the behavior of the energy losses and the engine efficiency for different MER.

As mentioned previously, the density of the fuel-air mixture for the non-diluted cases increases as MER increases. In these simulations, the initial pressure (1 bar) and initial temperature (40 °C) were held constant, so the total mass of working fluid increases, as shown in Fig. 4a. A linear trend line ($R^2 = 1$) can be used to represent that relationship. Fig. 4b presents the energy per unit mass of fuel-air mixtures. As can be seen, the stoichiometric hydrogen-air mixture has the highest specific energy, and hydrocarbons have a lower specific reactant energy. There is only a small difference in the specific reactant energy for hydrocarbons. The inlet energy can be easily calculated by multiplying the total mass with the specific energy of the reactants. Due to the increase of total reactant mass, the inlet energy increases with a higher MER fuel, as shown in Fig. 4c.

The specific heat ratio γ of the working fluids at the initial condition is presented in Fig. 4d. A more complex fuel (higher MER) causes a drop in γ. This can be explained by the increase of the molecule's degree of freedom and a lower mass fraction of air (mass based A/F_{st} in Table 1).

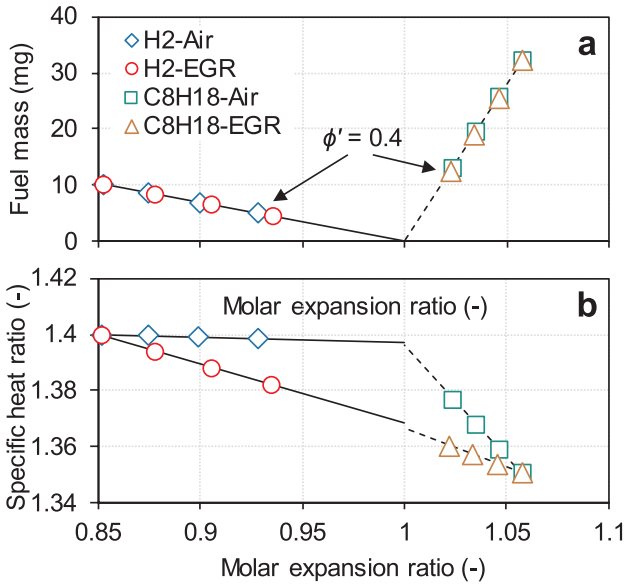

Fig. 5. Fuel mass and reactant's specific heat ratio for air and EGR dilution of hydrogen and iso-octane.

A similar behavior of the reactant mass was found for the user-defined fuels, the total mass (or mixture density) increases linearly with increased MER ($R^2 = 1$). Because of a similar mass based A/F_{st} ratio and the same LHV, the fuel mass and inlet energy also increase linearly with an increase in MER (with a constant starting pressure). Therefore, in order to maintain the inlet energy in the second option for user-defined fuels, the fuel's LHV was decreased linearly (from 44.6 MJ/kg for C_2H_4) with increased MER.

Fig. 5 presents the fuel mass (Fig. 5a) and the specific heat ratio (Fig. 5b) as a function of MER for H_2 and C_8H_{18} with air and EGR dilution. Because hydrogen has a MER less than unity, the MER increases as the dilution fraction increases. For iso-octane, MER decreases as the dilution increases. As can clearly be seen, at the same $\phi' = 0.4$ for each fuel, the two dilution cases have different fuel mass and MER, i.e. different inlet energy. In other words, ϕ' is not a good measure to represent the inlet energy of diluted mixtures for fuels with MER ≠1, contrary to what was suggested in [27,25]. The relationship between fuel mass and MER for both types of dilution, can be well presented by a linear line for each fuel. The fuel mass equals 0 when MER reaches 1 (only air or only burned gases). For each fuel, air dilution and EGR dilution have the same fuel mass (or inlet energy) at the same MER. The comparison between air dilution and EGR dilution at the same MER is thus preferable. For a fuel with MER equals unity, like CH_4 and C_2H_4, ϕ' could be employed also.

The specific heat ratio for both types of dilution and the two fuels also is presented in Fig. 5. For the air dilution of hydrogen, the working fluid contains only hydrogen and air, therefore, γ remains around 1.4. Hydrogen has a (slightly) higher γ compared to air; therefore, γ slightly decreases with the increase of air dilution. In the EGR dilution case, γ decreases significantly with dilution due to the increase of the water fraction in the mixture.

A different behavior was found for iso-octane where γ increases with dilution. In the air dilution case, γ tends towards the value of air with the increase of dilution. It reaches the same value as the air dilution cases of hydrogen at MER equals unity, the γ of pure air. Due to the difference between combustion products for hydrogen and iso-octane, the specific heat ratio at MER = 1 for the EGR dilution case of these two fuels is not the same. For hydrogen, the products contain water and nitrogen. However, the combustion products of iso-octane include water, carbon dioxide and nitrogen. This results in a difference in the specific heat ratio of the EGR dilution case between H_2 and C_8H_{18}

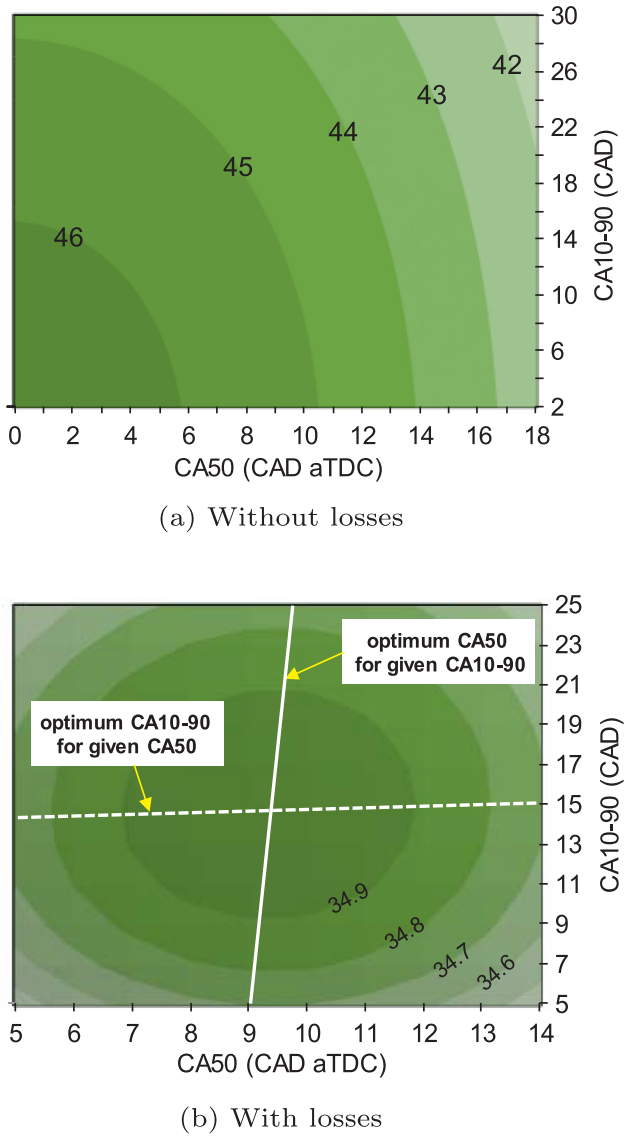

(a) Without losses

(b) With losses

Fig. 6. Contour plot of (a) engine efficiency without losses and (b) brake thermal efficiency as a function of CA50 and CA10-90 for a stoichiometric iso-octane engine. The solid line presents the optimum CA50 for a given value of CA10-90. The dashed line shows the optimum CA10-90 for a given value of CA50.

at MER = 1.

4. Engine simulation results and discussions

In this part, the simulation results are presented and analyzed. First, the results of non-diluted cases for standard fuels and user-defined fuels are analyzed to understand the impact of MER on energy losses and engine efficiency. The interaction between MER and compression ratio then is also illustrated. Based on these results, a recommendation for future fuel design is made. Finally, the comparison between air and EGR dilution is performed for both hydrogen and iso-octane.

4.1. Non-diluted combustion

4.1.1. Standard fuels

Fig. 6a presents the contour plot of engine efficiency without losses (Fig. 6a) and brake thermal efficiency (Fig. 6b) as a function of CA50 and CA10-90 for a stoichiometric iso-octane engine. In Fig. 6a, the value at bottom left corner (a CA50 at TDC and a CA10-90 of 2 CAD) represents the Otto cycle efficiency. With a later CA50 and/or longer CA10-90, the efficiency decreases due to the increase of combustion phasing loss and the increase of compression work. After taking heat transfer and friction work into account, the brake thermal efficiency (BTE) can be predicted. A short CA10-90 and an early CA50 result in lower efficiency because of the increase in heat transfer and friction losses. Fig. 6b presents the BTE in a CA50-CA10-90 domain. Due to the trade-off between combustion phasing loss and heat/friction losses, BTE reaches its peak at a later CA50 and a longer CA10-90 compared to the case without losses (Fig. 6a). The solid line shows the optimum CA50 for a given value of CA10-90. As can clearly be seen, the combustion phasing needs to be retarded with increasing combustion duration to have the highest efficiency. A longer combustion duration requires a later CA50 to reduce the compression work.

The difference in BTE is very small for different CA50 and CA10-90 within the investigated range. Varying CA50 and CA10-90 has a strong effect on the maximum pressure as well as the cylinder pressure at the end of the expansion stroke. Therefore, the exhaust pressure is influenced by the combustion as well. The actual impact of combustion phasing and combustion duration on engine efficiency might be more obvious if the pumping work is taken into account.

For a given CA50, the CA10-90 also influences engine efficiency. If the combustion duration is too long or too short, the efficiency decreases due to the reduction of expansion work and the increase of energy losses, respectively. The dashed line in Fig. 6b presents the optimum CA10-90 for a given value of CA50. The intersection point between these two lines is the point which has maximum engine efficiency.

Fig. 7 shows an example of engine efficiency for iso-octane as a function of CA50 combustion phasing. The combustion duration CA10-90 was optimized for each CA50 in order to achieve the maximum BMEP, as shown in the heavy dashed line in Fig. 6b. The effects of a change in LBV and in-cylinder turbulence with crank angle are not considered here. The uppermost solid line represents the Otto cycle efficiency (without losses). Because the combustion phasing for the Otto cycle is fixed at TDC, the Otto cycle efficiency is independent of CA50. The three lower lines show the efficiency with the same CA50 and CA10-90. The second line shows the efficiency without heat transfer and friction. The third line presents the gross indicated thermal efficiency (ITE), i.e. accounting for heat loss. The bottom most line represents the (gross) BTE (after taking friction into account).

As can clearly be seen, the combustion phasing loss increases with retarded CA50, i.e. the degree of constant volume combustion decreases. In order to reduce this loss, the combustion phasing needs to be advanced. Obviously, advancing CA50 is not always possible due to the

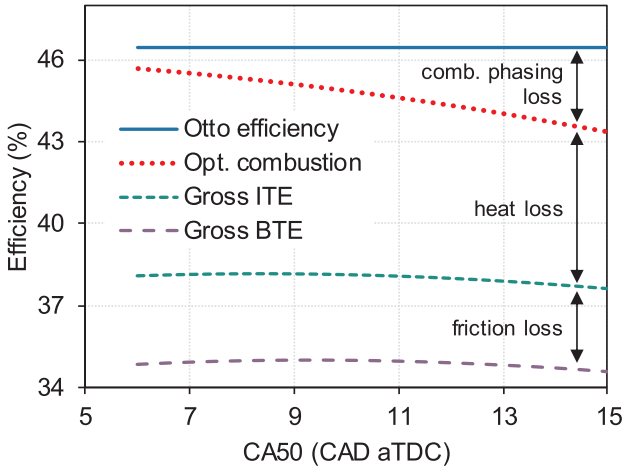

Fig. 7. Key efficiency loss as a function of combustion phasing CA50 for iso-octane.

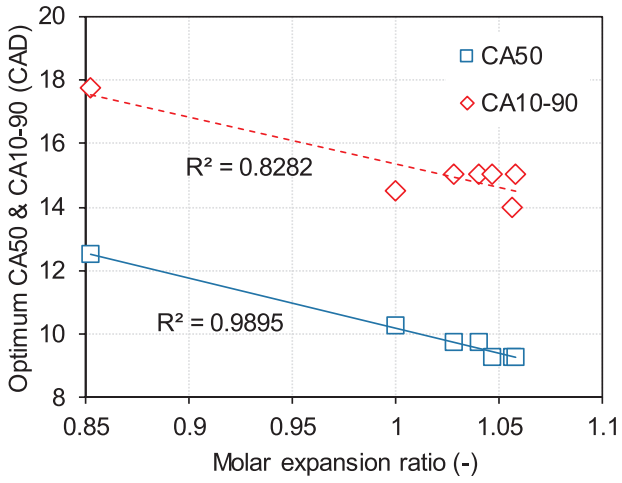

Fig. 8. Optimized CA50 and CA10-90 for standard fuels as a function of molar expansion ratio.

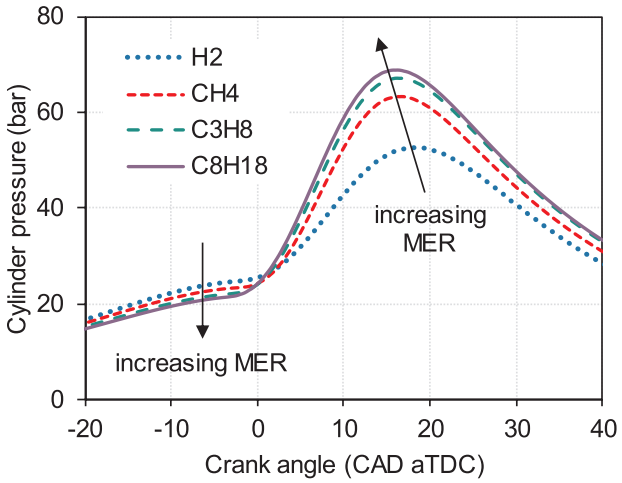

Fig. 9. Cylinder pressure histories versus crank angle at optimized CA50 and CA10-90 for four selected fuels: hydrogen, methane, propane and iso-octane.

auto-ignition of the end gas, or engine knock. Advanced CA50 and/or shorter CA10-90 also causes an increase in heat transfer and friction loss due to the increase of T_{gas} and P_{max}, see Eqs. (5) and (6). As shown in Fig. 7, the heat loss and friction loss decrease with retarded CA50. The optimized CA50 is determined as the timing which has the lowest total loss (combustion phasing + heat + friction).

The optimal CA50 is fuel-dependent because each fuel has a different combustion temperature and pressure, which results in different HTMEP and FMEP. Depending on the behavior of heat transfer and friction work, different fuels will have different optimized CA50 (and optimized CA10-90). For instance, the BTE reaches its peak at CA50 of 9.25 CAD aTDC for iso-octane.

Fig. 8 illustrates the optimum CA50 and CA10-90 for different fuels as a function of MER. A general trend for both parameters can clearly be seen, namely an earlier CA50 and shorter CA10-90 for a higher MER fuel. As mentioned before, the influence of the fuel's LBV is not considered in this work. Although hydrogen (MER = 0.852) in reality has the fastest LBV, this simplified approach shows that it would benefit from the longest CA10-90. As shown in Fig. 7, retarding CA50 results in a lower relative heat transfer and relative friction work. Low MER fuels have higher relative energy losses, thus the optimum CA50 is retarded for low MER fuels.

As shown in Eq. (5), the heat loss depends strongly on the maximum bulk gas temperature T_{gas}. Hydrogen has the highest combustion temperature because of the highest unburned gas temperature after compression (see Fig. 1) and the highest specific reactant energy (see Fig. 4b). Therefore, the HTMEP for hydrogen is higher than for other fuels. For hydrocarbons, the HTMEP is more or less the same. The relative heat loss is determined as the ratio of HTMEP to FuelMEP. Hydrogen has the highest HTMEP and the lowest FuelMEP, this means that this fuel has the highest relative heat loss, as also confirmed in reality [28]. Due to an increased FuelMEP for a higher MER hydrocarbon fuel, the relative heat loss decreases as MER increases.

The FMEP is calculated as a function of P_{max} following Eq. (6), so FMEP increases as P_{max} increases. Higher MER results in an increase in P_{max} [17], thus FMEP increases with a higher MER fuel. However, the increase in FuelMEP is more significant with increasing MER (see Fig. 4c). Thus, the relative friction work slightly decreases as the MER increases. These behaviors of energy losses explain the reason why higher MER fuels have an earlier optimum CA50 and shorter optimum CA10-90.

Fig. 9 presents the in-cylinder pressure profiles of four selected fuels as a function of crank angle at the optimized CA50 and CA10-90 for each fuel. The compression starts at the same initial pressure of 1 bar; however, the motored pressure decreases as MER increases due to the reduction of the specific heat ratio (see Fig. 4d). A more complex fuel has a lower compression work. Although the motored pressure decreases, the peak pressure increases with increased MER. This is a result of advanced CA50, higher FuelMEP, and higher MER. Thus, a more complex fuel has a higher expansion work.

The Otto cycle efficiency and engine efficiency including losses, as a function of MER, are presented in Fig. 10 for all considered fuels. The Otto cycle efficiency is represented by square symbols, at the top of the Figure. Similar to a previous study [16], the Otto cycle efficiency increases with a more complex (higher MER) fuel. Lower efficiencies result from adding losses such as combustion phasing, heat transfer and friction loss. The three lower efficiencies are simulated results with optimized CA50 and CA10-90 for each fuel (see Fig. 8). The absolute difference between these efficiencies represents the relative energy losses. The linear trend lines are also presented in this Figure. The slope of these linear trend lines increases with the addition of energy losses due to a smaller relative energy loss for a high MER fuel.

Due to an advanced CA50, higher MER fuels have a smaller relative combustion phasing loss. As discussed earlier, the friction and the heat transfer also decrease as MER increases, which causes a more obvious impact of MER on the gross indicated thermal efficiency (ITE) and especially BTE. For instance, the absolute difference in Otto cycle efficiency between hydrogen and iso-octane is only 2.3%, but once the

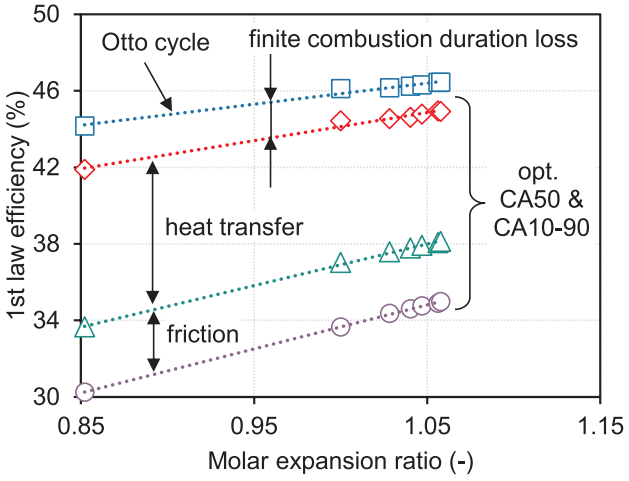

Fig. 10. Key first law efficiency losses for standard fuels as a function of molar expansion ratio. Opt. CA50 & CA10-90 for the traces including finite combustion duration, heat transfer and friction.

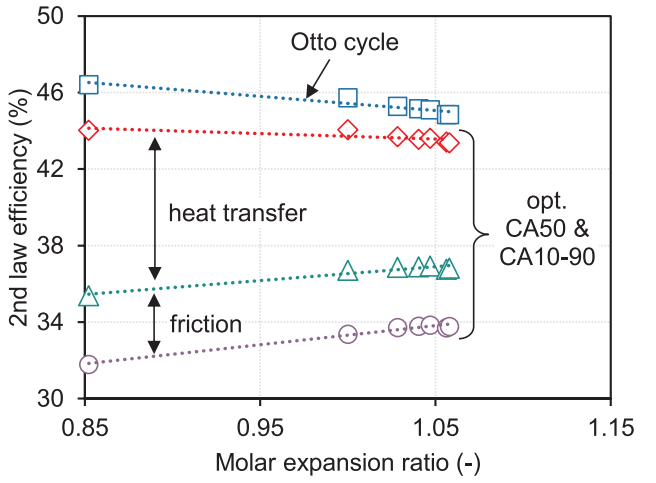

Fig. 11. Key second law efficiency losses for standard fuels as a function of molar expansion ratio. Opt. CA50 & CA10-90 for the traces including finite combustion duration, heat transfer and friction.

friction and heat transfer are considered, that difference more than doubles to 4.8% for the BTE.

The efficiency which is presented in Fig. 10 is based on the LHV, so it is termed a first law efficiency. The second law efficiency (exergy-based) was also calculated and is presented in Fig. 11. The fuel exergy is calculated based on the fuel's energy (or LHV) from GT-Power and the exergy-to-energy ratio from Szybist et al. [16]. As Szybist et al. [16] explain, exergy is a measure of a fuel's potential to do useful work because of physical and chemical differences between a system and the environment taking into consideration both the chemical changes in enthalpy and entropy during combustion, whereas first law energy content considers only enthalpy changes. Most fuels (including hydrocarbons) have an exergy-to-energy ratio larger than unity, so the second law efficiency is lower than the first law efficiency. Hydrogen has an exergy-to-energy ratio less than unity, thus the second law efficiency is higher. This causes a reverse trend in the Otto cycle efficiency from the first law results, it decreases as MER increases. After accounting for combustion phasing loss, the optimized combustion efficiency of hydrogen is still the highest. However, a similar behavior was found for the gross ITE and BTE, these efficiencies increase with improved MER. The difference in second law BTE between hydrogen and iso-octane is smaller than for the first law calculation.

4.1.2. User-defined fuels

In order to better isolate the impact of MER on engine efficiency, a series of user-defined fuels were investigated, shown in Table 1. All user-defined fuels have the same optimized CA50 and CA10-90, 9.25 CAD aTDC and 14 CAD, respectively. Fig. 12 shows the in-cylinder pressure and temperature for two fuels, C_2H_4 (MER = 1) and $C_{10}H_{20}$ (MER = 1.055). For $C_{10}H_{20}$, two cases were compared: constant LHV and constant FuelMEP (or constant inlet energy).

Because $C_{10}H_{20}$ is more complex than C_2H_4, it has molecular degrees of freedom which results in a lower γ. This results in a lower motored pressure and temperature for this fuel. Although $C_{10}H_{20}$ has a lower unburned gas temperature, the maximum combustion temperature of $C_{10}H_{20}$ is similar to that of C_2H_4 if the LHV is maintained (green dashed line in this Figure). This is due to the increase of cylinder pressure and the same specific reactant energy (same LHV and mass based A/F_{st}). Thanks to a higher MER and higher FuelMEP (or heat addition), the cylinder pressure in the expansion stroke is higher for $C_{10}H_{20}$. Higher pressure results in an increase in temperature.

For constant FuelMEP case (red dash-dotted line), the maximum combustion temperature for $C_{10}H_{20}$ is lower than the case for $C_{10}H_{20}$ with constant LHV and for C_2H_4. Compared to the case with constant

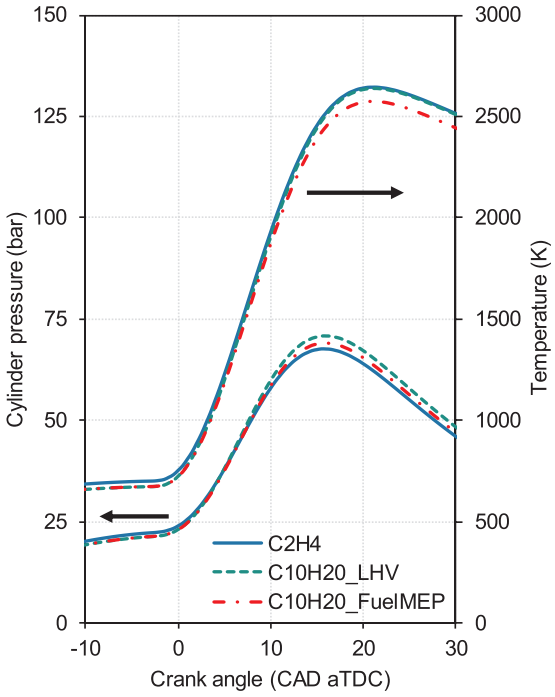

Fig. 12. In-cylinder pressure and temperature versus crank angle for three cases: C_2H_4, $C_{10}H_{20}$ with the same lower heating value, and $C_{10}H_{20}$ with the same inlet energy as other fuels.

LHV, the reduction of maximum temperature is due to the reduction of specific reactant energy and lower cylinder pressure. Compared to C_2H_4, although pressure slightly increases, lower unburned gas temperature and lower specific reactant energy cause a decrease in the combustion temperature. The peak pressure for $C_{10}H_{20}$ is higher than for C_2H_4 due to a higher MER. With lower compression work, higher expansion work and similar FuelMEP as C_2H_4, the BTE for $C_{10}H_{20}$ is higher.

Comparing the two cases, fixed LHV and fixed FuelMEP for $C_{10}H_{20}$, the relative combustion phasing loss is comparable. However, the latter case has a lower relative heat loss and a lower relative friction loss due to lower combustion temperature and lower peak pressure. Therefore, the BTE for the fixed FuelMEP case is higher than for the fixed LHV case. Fig. 13 shows the normalized BTE (normalized to ethylene, MER = 1) versus MER for the full series of C_nH_{2n} user-defined fuels investigated. As can be seen, the BTE increases relatively by ~0.9% with

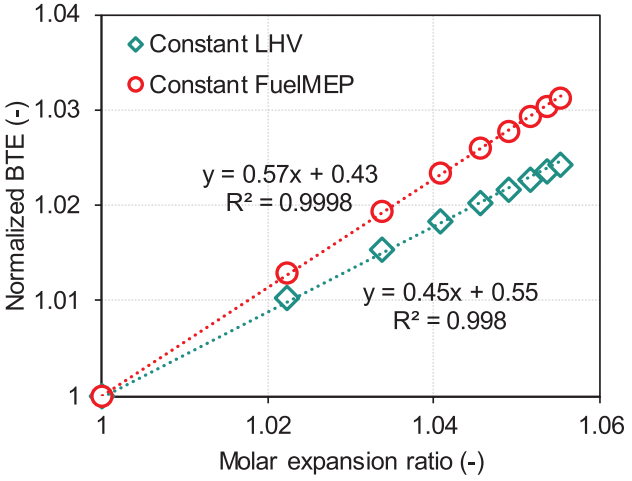

Fig. 13. BTE normalized to ethylene as a function of molar expansion ratio for user-defined fuels: fixed lower heating value and fixed inlet energy.

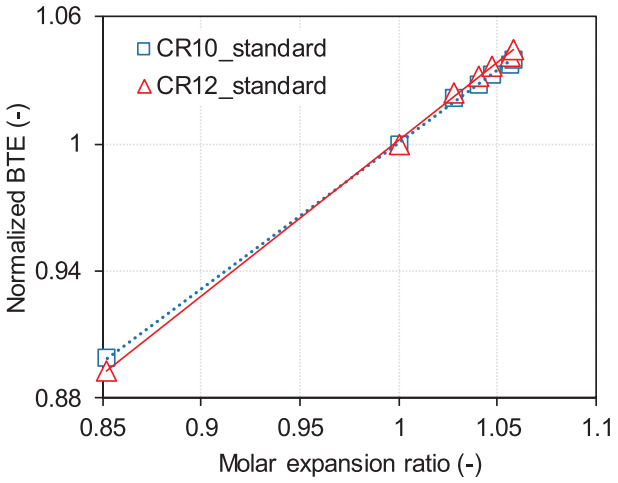

Fig. 14. BTE normalized to methane as a function of molar expansion ratio for standard fuels at the two compression ratios: 10:1 and 12:1.

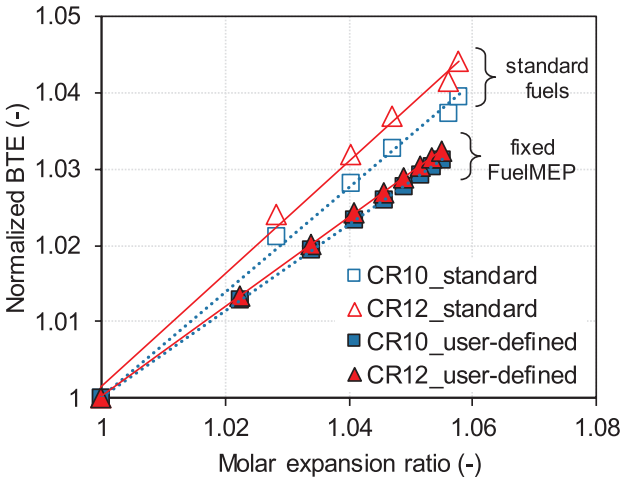

Fig. 15. BTE normalized to methane and ethylene as a function of molar expansion ratio for standard and user-defined fuels at the two compression ratios: 10:1 and 12:1.

an increase of 0.02 in MER (compared to the reference fuel, C_2H_4) for the fixed LHV case. For fixed FuelMEP, the relative improvement in BTE is ~1.15% with an increase of 0.02 in MER. The relative improvement will change with different initial temperature/pressure as well as compression ratio. Hence, we will now look at the impact of a change in compression ratio.

4.2. Impact of compression ratio

In order to see the interaction between MER and compression ratio, an additional simulation was performed at a CR of 12:1 with the same engine configuration, first for the standard fuels. The optimized CA50 and CA10-90 for all fuels were determined to achieve maximum BTE at this CR. The BTE increases with a higher CR for all fuels. To determine the effect of MER, the BTE for each fuel is normalized to that of methane and shown as a function of MER in Fig. 14. The first law efficiency is presented. Interestingly, the impact of MER is more obvious at higher CR, i.e. giving a higher relative improvement, for a fuel with MER greater than unity, and vice versa for a fuel with a MER less than 1.

To better understand this, we will now use the analysis of Wissink et al. [26], who have rewritten the pressure derivative, $dp/d\theta$, in terms of the contributions due to heat addition, $\dot{Q}$, volume change, $dV/d\theta$, mass addition, $dm/d\theta$, and molecular weight change, $dM/d\theta$, as

$$\frac{dp}{d\theta} = \left(\frac{dp}{d\theta}\right)_{\dot{Q}} + \left(\frac{dp}{d\theta}\right)_{V} + \left(\frac{dp}{d\theta}\right)_{m} + \left(\frac{dp}{d\theta}\right)_{M} \tag{9}$$

where

$$\left(\frac{dp}{d\theta}\right)_{\dot{Q}} = \left(\frac{\gamma - 1}{\gamma}\right)\dot{Q} \tag{10}$$

$$\left(\frac{dp}{d\theta}\right)_{M} = -\frac{p}{M}\frac{dM}{d\theta} \tag{11}$$

Because of mass conservation, the change in molecular weight depends on the change of the number of moles. For a fuel with MER $>$ 1, the number of moles of products is higher than that of the reactants. Therefore, $dm/d\theta$ is always negative for a fuel with MER $>$ 1 and positive for a fuel with MER $<$ 1 (hydrogen). A higher pressure p in Eq. (11) causes a positive contribution to $dp/d\theta$ for a fuel with MER $>$ 1 and vice versa for a fuel with MER $<$ 1. This explains the behavior of normalized BTE at higher CR, as in Fig. 14.

However, the impact of heat addition is also taken into account for standard fuels, as shown in Eq. (10). Therefore, the simulation then was performed for the user-defined fuels with fixed FuelMEP, to neglect that effect. Fig. 15 shows the normalized BTE (to that of fuels which have MER that equals unity, CH_4 and C_2H_4) versus MER. As can be seen, the relative improvement in BTE is smaller without the heat addition impact (for the user-defined fuels with fixed FuelMEP). The difference between normalized BTE at two compression ratios is smaller for user-defined fuels. For the standard fuels, the increase of $\dot{Q}$ in Eq. (10) results in a larger improvement. The results in this Figure further confirm that the impact of MER is more distinct at higher CR for fuels with MER larger than unity.

4.3. Diluted combustion

In this section, the impact of MER is analyzed for diluted combustion. Two fuels (H_2 and C_8H_{18}) were diluted by excess air (lean burn) and by burned gases (or EGR) at three ϕ': 0.8, 0.6 and 0.4. The initial pressure and temperature were maintained at 1 bar and 40 °C, thus the fuel mass and fuel energy decreases with increasing dilution levels. Similar to previous simulation, optimized CA50 and CA10-90 for each case (fuel, type of dilution, and ϕ') were used. The compression ratio is 10:1. As presented in a previous section, ϕ' is not a good measure to represent the specific inlet energy for diluted combustion for a fuel with MER $\neq$ 1. Therefore, the engine efficiencies for air and EGR dilution will be compared versus MER instead.

The Otto cycle efficiency and BTE for two fuels and two types of dilution are plotted against MER in Fig. 16. MER increases as dilution ratio increases for hydrogen, and vice versa for iso-octane. MER equals unity with 100% dilution (air or combustion products). As shown in this Figure, Otto cycle efficiency increases linearly as dilution ratio increases for both fuels. Although air and EGR dilution have the same inlet energy at the same MER (for a specific fuel), the efficiency for air dilution is higher than for EGR dilution. The efficiency tends towards the air cycle and EGR cycle efficiencies with dilution (see the end of the linear trend lines for both fuels/dilution types at MER = 1).

The air cycle and EGR cycle efficiencies can be calculated using Eq. (12). The difference in specific heat ratio between air and burned gases results in the difference in the air cycle and EGR cycle efficiencies. Combustion products contain a higher fraction of triatomic gases (CO_2 and/or H_2O), thus the specific heat ratio for the combustion products is lower than for air which contains only diatomic gases. Therefore, the air cycle has a higher Otto efficiency than the EGR cycle. Thanks to higher efficiency at MER of 1 for air dilution and the same efficiency for stoichiometric combustion, the Otto cycle efficiency for air dilution is higher than for EGR dilution at the same MER. The value of γ for air and EGR cycle in Eq. (12) depends on compression ratio and initial

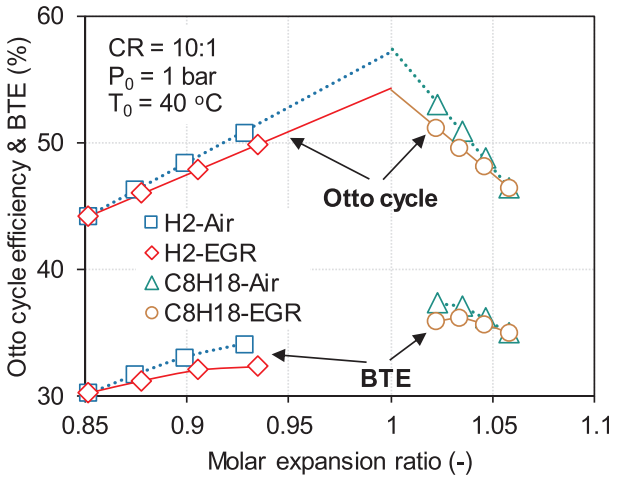

Fig. 16. Otto cycle efficiency and BTE as a function of molar expansion ratio for air/EGR dilution of hydrogen and iso-octane.

temperature.

$$\eta_{Otto} = 1 - \frac{1}{CR^{\gamma-1}} \tag{12}$$

Similar to the Otto cycle efficiency, BTE for air dilution is higher than for EGR dilution. Note that the impact of LBV on combustion duration is not taken into account. The optimized CA50 and CA10-90 for each mixture were used. As can be seen in Fig. 16, the BTE increases and then decreases with a rising of dilution ratio. The reduction of BTE at high dilution ratio can be explained by the increase of total energy losses. The increase of friction work is the main energy loss, which dominates the rising of Otto cycle efficiency [13,25]. As shown in Fig. 5a, inlet fuel mass (or inlet energy) decreases with rising dilution ratio, so the maximum pressure decreases. As shown in Eq. (6), the FMEP does not decrease proportionally with the peak pressure (or load). Because of a higher improvement in Otto efficiency for air dilution, the BTE for air dilution will reach its maximum at a higher dilution ratio. If engine load is maintained constant instead of the initial pressure and temperature, the results of FMEP and heat transfer may change these trends.

In reality, the combustion duration for air dilution is also shorter due to a faster LBV at the same ϕ' [29,30], so the efficiency for air dilution is higher than for EGR dilution. However, the low NO_x conversion of the three-way catalyst for lean conditions is the biggest challenge for the application of this strategy [29].

4.4. Future fuel design

The analyses described in the previous section help to give some pointers about promising fuels for future SI engines. Fuels should have a MER as high as possible, to increase engine efficiency. The benefit of high MER is more obvious with a higher compression ratio. The ideal fuel should thus be a fuel having high MER as well as good knock resistance. Also, if surrogate mixtures are sought to represent actual gasoline, next to matching thermo-physical and -chemical properties, and kinetic behavior, the MER should also be matched.

Based on Eq. (1), decreasing the number of carbon atoms and increasing the number of hydrogen and oxygen atoms causes an increase in MER. The MER of a fuel is very sensitive to a change of the number of oxygen atoms. Light alcohols like methanol (MER = 1.061) and ethanol (MER = 1.065) seem a good candidate because of a high MER combined with a good knock resistance. The mass based A/F_{st} of alcohol increases as MER increases (a reversed behavior compared to hydrocarbons). This results in higher specific reactant energy for lighter alcohols, so lower relative energy losses. Furthermore, as shown in Fig. 13, the efficiency improvement is more clear with lower LHV fuels (at the same MER). Together with other beneficial chemical and physical properties [31], light alcohols seem to be a very promising fuel for future SI engines.

A fuel with more oxygen atoms has a higher MER, e.g. ethyl acetate ($C_4H_8O_2$) with a MER of 1.08 and dimethyl carbonate ($C_3H_6O_3$) with a MER of 1.13. Engine efficiency depends not only on MER, but also on other fuel properties. Designing a fuel with high MER and good properties (e.g. high anti-knock quality, high LBV, high HoV, etc.) can reduce the CO_2 emissions from spark-ignition engines.

5. Conclusions

A simulation study has been carried out to evaluate the impact of the fuel's molar expansion ratio (MER) on engine efficiency. The simulation was performed using GT-Power with a Wiebe combustion model. A CA50 at top dead center and a CA10-90 of 2 degrees crank angle were first employed to represent isochoric combustion in the Otto cycle. For the other cases, the optimized CA50 locations and CA10-90 durations were used to achieve the maximum BMEP. The simulation was from −180 to +180 CAD aTDC, with the same initial conditions for the fuel-air mixture. Standard fuels and user-defined fuels with different MER were tested at the stoichiometric condition. For air and EGR dilution, the simulation was done for hydrogen and iso-octane. Based on the simulated results, several conclusions regarding engine efficiency can be drawn.

- First law Otto cycle efficiency increases with a higher MER fuel. The relative energy losses decrease as MER increases. After taking these energy losses into account, the improvement in the BTE is more obvious than in the Otto cycle efficiency.
- Second law Otto efficiency decreases as MER increases. Similar to the first law efficiency, the relative energy losses decrease as MER increases, which results in an increase in the BTE with increased MER. However, the improvement in the second law BTE is not as obvious as the improvement in the 1st law BTE with enhanced MER.
- The impact of A/F_{st} and heat addition was decoupled using user-defined fuels. Although the pre-combustion pressure is lower with higher MER fuels, higher MER causes an increase in the peak cylinder pressure. Compared to the fuel with MER of 1, the BTE increases ~1.15% for each increase of 0.02 of MER.
- The Otto cycle efficiency for air dilution is higher than for EGR dilution at the same MER.
- The impact of MER on engine efficiency is more obvious at a higher compression ratio for a fuel with MER greater than unity and vice versa for fuel with MER less than unity.

Additionally, the impact of MER on fuel properties and combustion can be made as follows:

- The reactant density increases as MER increases, resulting in higher total mass and higher inlet energy when the initial pressure and temperature are held constant. The specific heat ratio of the working fluid decreases as MER increases.
- In the case of constant intake pressure, fuel-to-charge equivalence ratio ϕ' is not a good measure to represent the specific energy of the reactant for a fuel with non-unity MER. For a specific fuel, the fuel mass in the air and EGR diluted cases is identical at the same MER.
- For hydrogen, the specific heat ratio decreases with the increase of dilution fraction. However, the specific heat ratio increases with increased dilution ratio for iso-octane. At the same MER, an air diluted mixture always has a higher specific heat ratio compared to an EGR diluted case.
- Compared to lower MER fuels, a higher MER fuel has an advanced optimum CA50 and a shorter optimum CA10-90. Compression work decreases and expansion work increases with increased MER.

- Future fuels should be designed to have a MER as high as possible and a good anti-knock quality.

In this study, the effect of pumping work was ignored. At part loads (where SI engines operate most under the real driving cycle), pumping work is one of the main losses. The impact of this loss needs to be taken into account in future work to predict the brake mean effective pressure and brake thermal efficiency. Experimental studies are also needed to evaluate the influence of MER on engine efficiency.

6. Disclaimer

This manuscript has been authored in-part by UT-Battelle, LLC, under Contract No. DE-AC0500OR22725 with the US Department of Energy (DOE). The US government retains and the publisher, by accepting the article for publication, acknowledges that the US government retains a nonexclusive, paid-up, irrevocable, worldwide license to publish or reproduce the published form of this manuscript, or allow others to do so, for US government purposes. DOE will provide public access to these results of federally sponsored research in accordance with the DOE Public Access Plan (http://energy.gov/downloads/doe-public-access-plan).

Declaration of Competing Interest

The authors declare that they have no known competing financial interests or personal relationships that could have appeared to influence the work reported in this paper.

Acknowledgments

The financial supports from the Special Research Fund (BOF) of Ghent University (Grant No. 01N03013) and GOA project (BOF16/GOA/004) are gratefully acknowledged.

The authors also acknowledge the support of the US Department of Energy Vehicle Technologies Office, particularly program managers Gurpreet Singh and Mike Weismiller.

References

[1] De Cesare M, Cavina N, Paiano L. Technology comparison for spark ignition engines of new generation. SAE Int J Engines 2017;10(5):2513–34. https://doi.org/10.4271/2017-24-0151.
[2] Miles P. Efficiency merit function for spark ignition engines: revisions and improvements based on FY16-17 research [Tech. rep.]. U.S. Department of Energy, DOE/GO-102018-5041; 2018.
[3] Boot MD, Tian M, Hensen EJ, Sarathy SM. Impact of fuel molecular structure on auto-ignition behavior–design rules for future high performance gasolines. Prog Energy Combust Sci 2017;60:1–25. https://doi.org/10.1016/j.pecs.2016.12.001.
[4] ASTM D2699-19. Test method for research octane number of spark-ignition engine fuel. West Conshohocken, PA: ASTM International; 2019.
[5] ASTM D2700-19. Test method for motor octane number of spark-ignition engine fuel. West Conshohocken, PA: ASTM International; 2019.
[6] Kalghatgi G. Fuel anti-knock quality–part I. Engine studies. SAE Technical Paper 2001-01-3584 2001. https://doi.org/10.4271/2001-01-3584.
[7] Prakash A, Wang C, Janssen A, Aradi A, Cracknell R. Impact of fuel sensitivity (RON-MON) on engine efficiency. SAE Int J Fuels Lubricants 2017;10(1):115–25. https://doi.org/10.4271/2017-01-0799.
[8] Remmert S, Campbell S, Cracknell R, Schuetze A, Lewis A, Giles K, Akehurst S, Turner J, Popplewell A, Patel R. Octane appetite: the relevance of a lower limit to the MON specification in a downsized, highly boosted DISI engine. SAE Int J Fuels Lubricants 2014;7(3):743–55. https://doi.org/10.4271/2014-01-2718.
[9] Szybist JP, Splitter DA. Pressure and temperature effects on fuels with varying octane sensitivity at high load in SI engines. Combust Flame 2017;177:49–66. https://doi.org/10.1016/j.combustflame.2016.12.002.
[10] Szybist JP, Splitter DA. Understanding chemistry–specific fuel differences at a constant RON in a boosted SI engine. Fuel 2018;217:370–81. https://doi.org/10.1016/j.fuel.2017.12.100.
[11] Cracknell R, Prakash A, Head R. Influence of laminar burning velocity on performance of gasoline engines. SAE Technical Paper 2012-01-1742 2012. https://doi.org/10.4271/2012-01-1742.
[12] Kolodziej CP, Pamminger M, Sevik J, Wallner T, Wagnon SW, Pitz WJ. Effects of fuel laminar flame speed compared to engine tumble ratio, ignition energy, and injection strategy on lean and EGR dilute spark ignition combustion. SAE Int J Fuels Lubricants 2018;10(1):82–94. https://doi.org/10.4271/2017-01-0671.
[13] Nguyen D-K, Stepman B, Vergote V, Sileghem L, Verhelst S. Combustion characterization of methanol in a lean-burn direct injection spark ignition (DISI) engine. SAE Technical Paper 2019-01-0566 2019. https://doi.org/10.4271/2019-01-0566.
[14] Szybist JP, Splitter D. Effects of fuel composition on EGR dilution tolerance in spark ignited engines. SAE Int J Engines 2016;9(2):819–31. https://doi.org/10.4271/2016-01-0715.
[15] ASTM D4809-18. Standard test method for heat of combustion of liquid hydrocarbon fuels by bomb calorimeter (precision method). West Conshohocken, PA: ASTM International; 2018.
[16] Szybist JP, Chakravathy K, Daw CS. Analysis of the impact of selected fuel thermochemical properties on internal combustion engine efficiency. Energy Fuels 2012;26(5):2798–810. https://doi.org/10.1021/ef2019879.
[17] Nguyen D-K, Sileghem L, Verhelst S. Exploring the potential of reformed-exhaust gas recirculation (R-EGR) for increased efficiency of methanol fueled SI engines. Fuel 2019;236:778–91. https://doi.org/10.1016/j.fuel.2018.09.073.
[18] Gamma Technologies. GT-suite version 7.5 user's manual. Westmont, IL, USA: Gamma Technologies; 2015.
[19] Lam N, Tuner M, Tunestal P, Andersson A, Lundgren S, Johansson B. Double compression expansion engine concepts: a path to high efficiency. SAE Int J Engines 2015;8:1562–78. https://doi.org/10.4271/2015-01-1260.
[20] Nguyen D-K, Van Craeynest T, Pillu T, Coulier J, Verhelst S. Downsizing potential of methanol fueled DISI engine with variable valve timing and boost. SAE Technical Paper 2018-01-0918 2018. https://doi.org/10.4271/2018-01-0918.
[21] Ahmed A, Waqas M, Naser N, Singh E, Roberts W, Chung S, Sarathy M. Compositional effects of gasoline fuels on combustion, performance and emissions in engine. SAE Int J Fuels Lubricants 2016;9(3):460–8. https://doi.org/10.4271/2016-01-2166.
[22] Heywood JB. Internal combustion engine fundamentals. McGraw-Hill Publishing; 1988.
[23] Morel T, Keribar R. A model for predicting spatially and time resolved convective heat transfer in bowl-in-piston combustion chambers. SAE Technical Paper 850204 1985. https://doi.org/10.4271/850204.
[24] Chen SK, Flynn PF. Development of a single cylinder compression ignition research engine. SAE Technical Paper 650733 1965. https://doi.org/10.4271/650733.
[25] Lavoie GA, Ortiz-Soto E, Babajimopoulos A, Martz JB, Assanis DN. Thermodynamic sweet spot for high-efficiency, dilute, boosted gasoline engines. Int J Engine Res 2013;14(3):260–78. https://doi.org/10.1177/1468087412455372.
[26] Wissink ML, Splitter DA, Dempsey AB, Curran SJ, Kaul BC, Szybist JP. An assessment of thermodynamic merits for current and potential future engine operating strategies. Int J Engine Res 2017;18(1–2):155–69. https://doi.org/10.1177/1468087416686698.
[27] Lavoie GA, Martz J, Wooldridge M, Assanis D. A multi-mode combustion diagram for spark assisted compression ignition. Combust Flame 2010;157(6):1106–10. https://doi.org/10.1016/j.combustflame.2010.02.009.
[28] Demuynck J, Raes N, Zuliani M, De Paepe M, Sierens R, Verhelst S. Local heat flux measurements in a hydrogen and methane spark ignition engine with a thermopile sensor. Int J Hydrogen Energy 2009;34(24):9857–68. https://doi.org/10.1016/j.ijhydene.2009.10.035.
[29] Nguyen D-K, Verhelst S. Development of laminar burning velocity correlation for the simulation of methanol fueled SI engines operated with onboard fuel reformer. SAE Technical Paper 2017-01-0539 2017. https://doi.org/10.4271/2017-01-0539.
[30] Middleton RJ, Martz JB, Lavoie GA, Babajimopoulos A, Assanis DN. A computational study and correlation of premixed isooctane air laminar reaction fronts diluted with EGR. Combust Flame 2012;159(10):3146–57. https://doi.org/10.1016/j.combustflame.2012.04.014.
[31] Verhelst S, Turner JW, Sileghem L, Vancoillie J. Methanol as a fuel for internal combustion engines. Prog Energy Combust Sci 2019;70:43–88. https://doi.org/10.1016/j.pecs.2018.10.001.